This preprint is in final form. It appeared in:
J. Speidel (ed.), Neue Kommunikationsanwendungen in modernen Netzen
ITG-Fachbericht, Vol. 171, VDE Verlag, Berlin 2002, pp. 109–115

ISI/ICI COMPARISON OF DMT AND WAVELET BASED MCM SCHEMES FOR TIME–INVARIANT CHANNELS

Maria Charina, Kurt Jetter, Achim Kehrein, Götz E. Pfander, and Georg Zimmermann
Institut für Angewandte Mathematik und Statistik, Universität Hohenheim, D–70593 Stuttgart, Germany

Werner Kozek
Siemens AG Österreich, Programm- und Systementwicklung, A–1030 Vienna, Austria

ABSTRACT

We present analytical results, numerical estimates, and numerical simulations showing that wavelet based affine MCM schemes are unfit for communication through dispersive time invariant channels as given in DSL and some wireless communication environments. Currently used FFT based MCM schemes (DMT) outperform those based on wavelets regardless of which wavelet is chosen.

1. INTRODUCTION

Modern digital communication systems show a general trend towards linear modulation schemes [1]. Important examples of linear modulation among others are CDMA and OFDM (orthogonal frequency division multiplex). The common principle of these schemes is that the transmission signal can be written as a series expansion based on a prescribed set of "pulses" which are trigonometric polynomials in case of OFDM and binary sequences in case of CDMA. Other variants are the classical PAM or QAM modulation.
Any of these linear modulation schemes are part of standardized digital communication systems, either for wireless (e.g., HIPERLAN 2 in case of OFDM) or wired (e.g. ADSL, where the baseband variant DMT of OFDM is standardized for the asymmetrical transmission over digital subscriber line) systems. We shall address one of the key questions in the design of future communication systems concerning the design of the transmission pulses in such a linear modulation scheme.
In principle any essentially time-limited and essentially band-limited function can be taken as starting point for the design of transmission signal sets. However, many practical side constraints have to be fulfilled in order to obtain realistic implementations and to enable the receiver to cope with the detrimental effects of the channel:

(i) The function system should be orthogonal, or at least linearly independent, in order to have unique demodulation.

(ii) The whole set of transmission pulses must have a structure which admits fast DSP algorithms for the implementation.

(iii) The function system must be robust with respect to the distortions caused by the channel.

The introduction of wavelets almost 20 years ago had a lasting effect on many fields in mathematics and engineering. For a detailed historical account see [5, 15]. In information and communication theory, wavelets have been successfully applied to source coding, e.g., JPEG 2000. Various authors have proposed the application of wavelet systems for modulation/signal synthesis also, e.g., see [4, 9, 16]. Even though wavelet families do fulfill the first two constraints for multicarrier modulation (MCM) mentioned above, they fail the third objective: perturbation stability when faced with the dispersive effect caused by a linear translation invariant operator. This failure leads to high ISI and ICI.
In this paper we shall present the problem of MCM from a mathematical point of view and outline our mathematical/technical results concerning the "perturbation stability of coherent Riesz-systems" [8] in Section 2 and Section 3. The emphasis of our proposed contribution is the comparison of shift invariant MCM systems based on numerical simulations. We shall present exemplary results of those simulations in Section 5.

2. SHIFT INVARIANT MULTICARRIER MODULATION

In linear multicarrier modulation systems the input signal is synthesized as a linear combination of basis functions $\{g_i(t)\}_{i\in I}$ (I denotes a possibly infinite index set), where the complex or real coefficients sustain the information aimed at transmission. In the case of *shift invariant* multicarrier modulation (Figure 1) the basis functions are translates of a finite family of functions $\{g_l(t)\}_{l=0,\dots,N-1}$, i.e., for some $T>0$ and $I=\{0,\dots,N-1\}\times\mathbb{Z}$ we have

$$g_{l,k}(t) = g_l(t-kT), \quad \text{for } l=0,\dots,N-1,\ k\in\mathbb{Z}.$$

Hence, the resulting information carrying input signal is given by

$$x(t) = \sum_{k=-\infty}^{\infty} x_k(t) = \sum_{k=-\infty}^{\infty}\sum_{l=0}^{N-1} c_{l,k}\ g_l(t-kT).$$

We assume throughout this work that the channel distortion due to transmission over a physical communication channel corresponds to a translation invariant system, i.e.,

$$(K_h\, x)(t) = (h{*}x)(t) = \int_{\mathbb{R}} h(t-t')\, x(t')\, dt'.$$

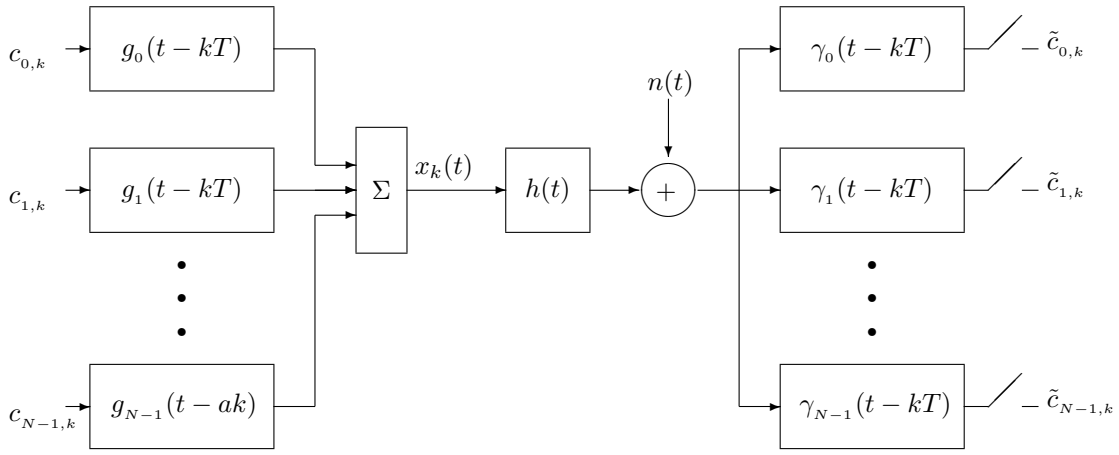

Fig. 1. Shift invariant multicarrier modulation

The transmitter strategy corresponds to a signal synthesis, accordingly the receiver performs a signal analysis, in the sense of matched filtering by a family of functions with identical structure $\gamma_{l,k}(t) = \gamma_l(t - kT)$:

$$\tilde{c}_{l,k} = \langle x * h, \gamma_{l,k} \rangle = \int_{\mathbb{R}} (x * h)(t)\, \overline{\gamma_{l,k}(t)}\, dt.$$

In order to guarantee the stable and effective transmission of the information contained in the sequence $\{c_{l,k}\} \in l^2(\{0, \ldots, N-1\} \times \mathbb{Z})$, the families $\{g_l(t)\}$ and $\{\gamma_l(t)\}$ need to satisfy the following conditions:

(i) $\{g_{l,k}(t)\}$ and $\{\gamma_{l,k}(t)\}$ are Riesz bases of their linear span to guarantee stability and continuity of the synthesis and analysis maps.

$$A \sum_{l,k} |c_{l,k}|^2 \leq \Big\| \sum_{l,k} c_{l,k} g_{l,k} \Big\|^2 \leq B \sum_{l,k} |c_{l,k}|^2$$

where $$\|x\|^2 = \int_{\mathbb{R}} |x(t)|^2 dt.$$

Note that finite-length, discrete-time signals establish a finite-dimensional Hilbert space. Here, the notion of a Riesz basis reduces to a set of N linear independent vectors of dimension N.

(ii) Biorthogonality of the families $\{g_{l,k}(t)\}$ and $\{\gamma_{l,k}(t)\}$, i.e.,

$$\langle g_{l,k}, \gamma_{l',k'} \rangle = \delta_{l,l'} \delta_{k,k'},$$

to ensure $c_{l,k} = \tilde{c}_{l,k}$ for all l, k, in case of an ideal channel $K = Id$.

(iii) The families $\{g_l(t)\}$ and $\{\gamma_l(t)\}$ should be structured to allow for fast synthesis and analysis algorithms.

(iv) Uniform compact support, i.e., $\operatorname{supp} g_l \subset [0, T]$, in order to restrict ISI and time delay.

(v) Efficient use of an assigned bandwidth.

(vi) Low ICI/ISI for an ensemble of convolution operators $\mathcal{H} \subset \mathcal{L}(L^2(\mathbb{R}))$, i.e., for all $h(t) \in \mathcal{H}$:

$$G^h_{l,k,l',k'} := \langle h * g_{l,k}, \gamma_{l',k'} \rangle \approx d_{l,k}\, \delta_{l,l'} \delta_{k,k'}. \tag{2.1}$$

The most prominent coherent function systems satisfying conditions i) - v) are Weyl–Heisenberg and wavelet systems which will be described in Section 4 and Section 5. The mentioned fast algorithms are based on the FFT, and on Mallat's cascade algorithm, respectively. For theoretical analysis of the ICI/ISI of MCM pulses, we consider a set $\mathcal{H}$ of absolutely integrable impulse responses $h(t)$ defined by the following requirements:

(i) The impulse response is supported within a centered interval of length t_0,i.e.,

$$\operatorname{supp} h \subseteq [-\tfrac{t_0}{2}, +\tfrac{t_0}{2}].$$

Although $h(t)$ does not have finite support in general, we may cut it off at some point and treat the influence of the remaining part as noise.

(ii) Assume that the first moment of the magnitude–squared impulse response vanishes (corresponding to properly defined timing recovery):

$$\int_{\mathbb{R}} |h(t)|^2\, t\, dt = 0.$$

(iii) The maximum of the magnitude transfer function is normalized (corresponding to perfect automatic gain control)

$$\sup_f |H(f)| = 1.$$

3. GENERAL RESULTS

To analyze the ICI/ISI of the pulses $\{g_{l,k}(t)\}$ independently of the analysis pulses $\{\gamma_{l,k}(t)\}$ we choose orthogonal perturbation as a measure of stability, i.e., we define

$$d_{g,h} = \big\| K_h g - P_{<g>}(K_h g) \big\|_{\boldsymbol{L}^2},$$

where $P_{<g>}$ is the orthogonal projection onto the span of $g(t)$, given by $P_{<g>}(K_h g)(t) = \frac{\langle K_h g, g\rangle}{\langle g, g\rangle}\, g(t)$ (cf., Figure 2).

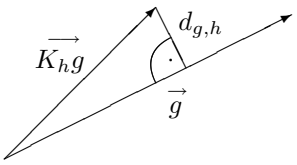

Fig. 2. Orthogonal distortion(=perturbation)

Note that if the family $\{\gamma_{l,k}(t)\}$ is orthonormal, the orthogonal perturbation of $g_{l,k}(t)$ is related to the ICI/ISI of the synthesis prototype $g_{l,k}(t)$ via

$$d^2_{g_{l,k},h} \geq \sum_{l'\neq l, k'\neq k} |G^h_{l,k,l',k'}|^2 = \sum_{l'\neq l, k'\neq k} |\langle h{*}g_{l,k}, \gamma_{l',k'}\rangle|^2.$$

In our treatise, we aim at finding lower and upper bounds on the orthogonal perturbation $d_{g,h}$ for all $h(t) \in \mathcal{H}$. For simplicity, we define

$$d_g = \sup_{h\in\mathcal{H}} d_{g,h}\,.$$

Since the convolution $K_h g(t) = h{*}g(t)$ corresponds to multiplication in the Fourier domain, d_g can be related to the frequency localization of $g(t)$, as the following theorem shows.

Theorem 1 (Upper bound) *For $g(t) \in \boldsymbol{L}^2(\mathbb{R})$ with $\|g\|_{\boldsymbol{L}^2} = 1$, we have*

$$d_g^2 \leq (\pi t_0)^2 \sigma^2_{|G|^2}\,,$$

where $\sigma^2_{|G|^2}$ is the variance of $|G|^2$, i.e.,

$$\sigma^2_{|G|^2} = \int_{\widehat{\mathbb{R}}} (f-\mu)^2\, |G(f)|^2\, df$$

with

$$\mu = \mu_{|G|^2} = \int_{\widehat{\mathbb{R}}} f\, |G(f)|^2\, df\,.$$

(Note that $G(f)$ denotes the Fourier transform of $g(t)$). On the other hand, one must expect that signals which are not well localized on the frequency side potentially undergo a relatively strong orthogonal perturbation.
Clearly, for a given convolution operator there might be arbitrarily bad localized functions $g(t)$ which are exact eigenfunctions of this specific operator, so $d_{g,h} = 0$ for this particular $h(t)$ — but for practical purposes, we require a family of basis functions that are stable under the action of all $h(t) \in \mathcal{H}$. Therefore, to be able to show that certain families are inadequate, we want to determine a lower bound for d_g. Using an uncertainty principle obtained by Slepian, Pollak, and Landau [11, 12, 13] we obtain the following result.

Theorem 2 (Lower bound) *There exist constants $s \in]0,1[$ and $r \in [\frac{1}{2}, 1[$ such that for $g(t) \in \boldsymbol{L}^2(\mathbb{R})$, $\|g\|_{\boldsymbol{L}^2} = 1$, with $\operatorname{supp} g \subseteq [\alpha, \alpha + T_g]$ for some $\alpha \in \mathbb{R}$ and $T_g > 0$, we have*

$$d_g^2 \geq r^2\Big(1 - \frac{4}{3}\, s\, \frac{T_g}{t_0}\Big) \qquad \text{for } \frac{T_g}{t_0} \leq \frac{1}{2s},$$

$$\text{and} \qquad d_g^2 \geq \frac{1}{12}\Big(\frac{r\, t_0}{s\, T_g}\Big)^2 \qquad \text{for } \frac{T_g}{t_0} > \frac{1}{2s}.$$

4. SPECIFIC MCM SCHEMES

We now proceed to apply these results to compare structured signal families of wavelet, Wilson, and Weyl–Heisenberg type with respect to their stability under convolution operators.
For numerical results based on Theorem 1 and Theorem 2 we assume $\operatorname{supp} h \subseteq [-\frac{t_0}{2}, +\frac{t_0}{2}]$ and $T = 50\, t_0$. Furthermore, we will use as realistic choice $r \doteq 0.9$ and $s \doteq 1$.
As for the number of elements N in the family, $N \geq 256$ seems realistic; in VDSL applications, $N \approx 2000$ is used.
Weyl–Heisenberg or *Gabor* systems [7] correspond to a rectangular tiling of the time–frequency plane, the $g_l(t)$ and $\gamma_l(t)$ are modulated versions of appropriately chosen prototype function $g_0(t)$ and $\gamma_0(t)$, i.e.,

$$g_l(t) = g_0(t) e^{2\pi i(\rho/T)lt}, \quad \gamma_l(t) = \gamma_0(t) e^{2\pi i(\rho/T)lt}\,.$$

Existence of Riesz bases requires [10]

$$\rho \geq 1.$$

Thus we have

$$\operatorname{supp} g_l = \operatorname{supp} g_0$$

and

$$|G_l(f)|^2 = |G_0(f - (\rho/T)l|^2.$$

Since the variance is translation invariant, we have

$$\sigma^2_{|G_l|^2} = \sigma^2_{|G_0|^2}$$

for all $g_l(t)$, so the upper bound from Theorem 1 holds uniformly in $h(t) \in \mathcal{H}$ and $l = 0 \ldots N{-}1$.
Using for $g_0(t)$ a triangle function, a trapezoidal function, or the polynomial $t^2(t{-}a)^2$ (properly normalized) yields

$$d_g^2 \doteq 0.0012\,.$$

It is worth emphasizing that the main property ensuring this uniform upper bound is the fact that within a Weyl–Heisenberg family, all $G_l(f)$ share the same frequency localization.
The real-valued *Wilson* bases are equivalent to the so–called OFDM/OQAM systems [2] and can be formu-

lated in terms of sin-components and cos-components:

$$\begin{aligned} g_0(t) &= g(t)\,, \\ g_{m,1}(t) &= g(t)\,\sqrt{2}\cos(2\pi\tfrac{2m}{T}t), \\ g_{m,2}(t) &= g(t-\tfrac{T}{2})\,\sqrt{2}\cos(2\pi\tfrac{2m-1}{T}t)\,, \\ g_{m,3}(t) &= g(t)\,\sqrt{2}\sin(2\pi\tfrac{2m-1}{T}t), \\ g_{m,4}(t) &= g(t-\tfrac{T}{2})\,\sqrt{2}\sin(2\pi\tfrac{2m}{T}t)\,, \end{aligned}$$

where the index set is defined as $m \in [0, M-1]$ and the corresponding number of pulses per symbol time is given by $N = 4M+1$. Similar to WH-Systems, modulation and demodulation can be realized efficiently via FFT. A recently developed theory allows the design of pulses $g(t)$ with improved frequency localization [2]. Nevertheless, the following theorem holds.

Theorem 3 *In a Wilson basis with at least 200 elements and* $\operatorname{supp} g_0 \subseteq [0,T]$*, there is an element* g_l *with*

$$d^2_{g_l} \geq \tfrac{r^2}{5} \doteq 0.16\,.$$

The popular dyadic *wavelet* bases [5, 16] are defined via

$$g_m^{(n)}(t) = 2^{m/2} g_0\big(2^m(t-n\tfrac{T}{2^m})\big)$$

where g_0 is an appropriate prototype function (referred to as mother wavelet) and the index set is defined as follows:

$$m = 0, 1, \ldots, M\,, \quad n = 0, 1, \ldots, 2^m-1,$$

(The total number of transmission pulses within symbol period T is accordingly given by $N = 2^{M+1}-1$)). In a dyadic wavelet basis, we encounter the problem that, since scaling on the time side results in reverse scaling on the frequency side, the frequency localization gets worse and worse as the indices grow. The following result gives a quantitative estimate of this effect.

Theorem 4 *In a dyadic wavelet family with* $\operatorname{supp} g_0 \subseteq [0, KT]$ *and finest scaling level* $M \geq 7 + \log_2(K)$*, the elements* $g_M^{(n)}(t)$ *on level* M *satisfy*

$$d^2_{g_M^{(n)}} \geq 0.81\,(1 - 67\cdot 2^{-M}K)\,.$$

When using the orthogonal Daubechies wavelet with four vanishing moments (db4 in MatLab), we may choose $K = 8$. If $N > 1024$, we need $M \geq 11$ which yields $d^2_{g_{11}^{(n)}} \geq 0.386$; for $N > 2048$ with $M \geq 12$ we obtain $d^2_{g_{12}^{(n)}} \geq 0.598$.

5. NUMERICAL SIMULATIONS

To corroborate our theoretical results of Section 3 in a realistic setup, we shall compute the effective channel matrix of an exemplary wavelet transmission basis and of an exemplary Weyl–Heisenberg transmission basis with respect to a normalized convolution operator reflecting a 2km, 0.4mm PE twisted copper wire cable. In order to visualize the channel matrices (2.1), we resort the synthesis and analysis families and display a segment of the biinfinite block Toeplitz matrix.
To compare the families discussed within a setting similar to ADSL, we choose $T \approx 250\mu$s and bases capable of transmitting about 500 real coefficients (250 imaginary coefficients) utilizing the baseband [-1,1] MHz.
The impulse response of a 2km, 0.4mm PE twisted copper wire cable sampled at 2 MHz has been calculated according to [6]. The resulting causal impulse response has been shifted to improve the performance of all the coherent families discussed here. Additionally, the impulse response has been normalized so that $\sup|H(f)| = 1$. The resulting function $h(t)$ is shown in Figure 3.

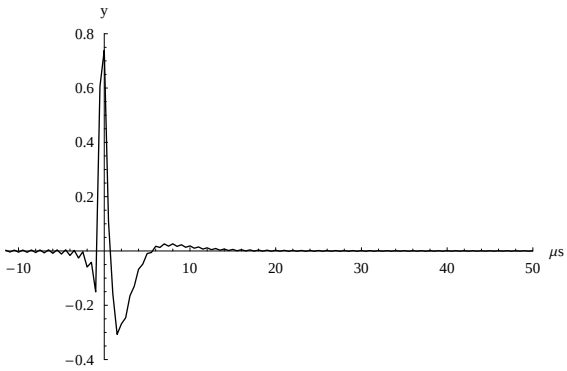

Fig. 3. Channel impulse response $h(t)$ of a 2km $0,4$mm PE twisted copper wire cable.

The colormap used in the Figures below is shown in 4.

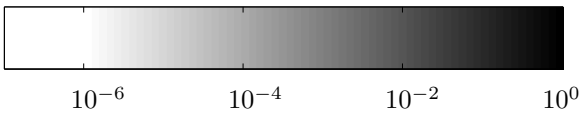

Fig. 4. Colormap used in the channel matrix images.

To illustrate the performance of an exemplary Weyl–Heisenberg system, we choose as prototype functions

$$g_0(t) = \gamma_0(t) = \frac{1}{\sqrt{250}}\,\chi_{[0,250)}(t\,[\mu\text{s}]).$$

Using $T = 250\mu$s, $b = \frac{1}{250}$MHz and $L = 250$, we obtain the channel matrix displayed in Figure 5. Details of this matrix are shown in Figure 6.
In the Weyl–Heisenberg example, we shall now employ a cyclic prefix of $30\mu s$. Hence, the prototype functions we choose

$$g_0(t) = \frac{1}{\sqrt{250}}\,\chi_{[-30,250)}(t\,[\mu\text{s}])$$

and

$$\gamma_0(t) = \frac{1}{\sqrt{250}}\,\chi_{[0,250)}(t\,[\mu\text{s}]).$$

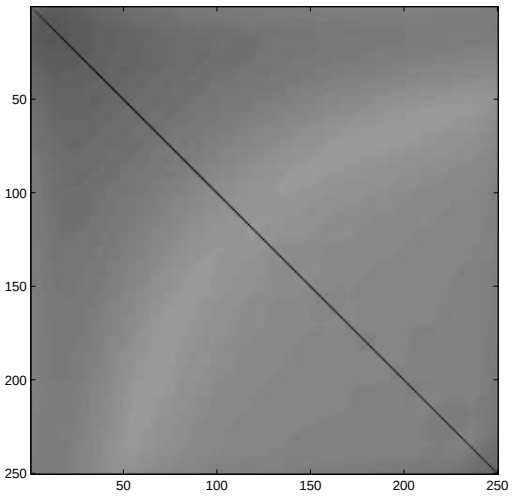

Fig. 5. Channel matrix of a Weyl–Heisenberg family.

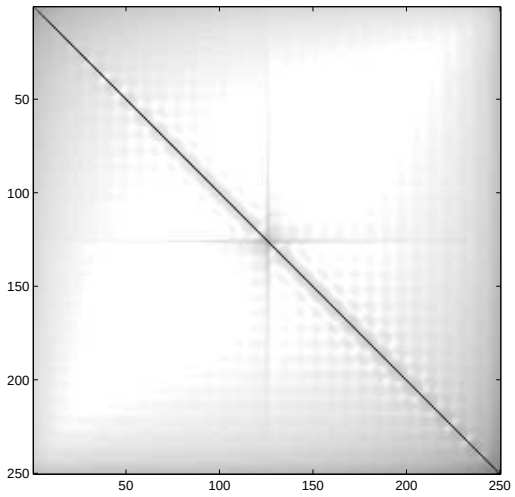

Fig. 7. Channel matrix of a Weyl–Heisenberg family using a *cyclic prefix*.

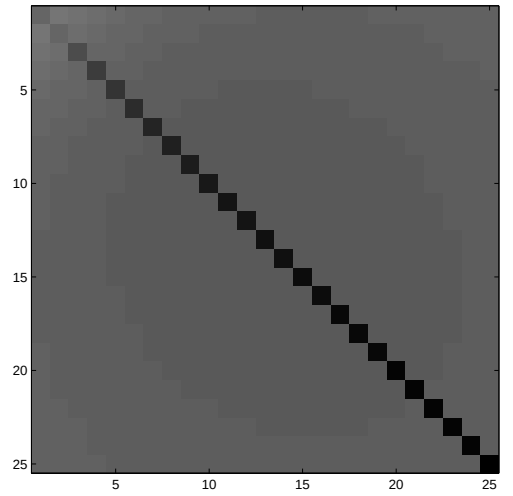

Fig. 6. Details of Figure 5.

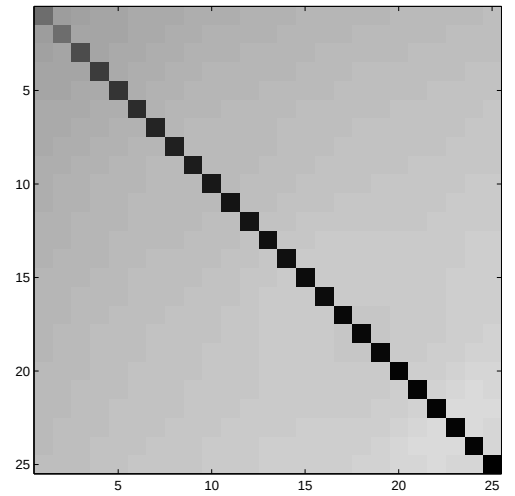

Fig. 8. Details of Figure 7.

Using $T = 280\mu$s, and $L = 250$, we obtain the segments of the channel matrix displayed in Figure 7 and in Figure 8. Note that we do not have exact diagonalization, since the duration of the *cyclic prefix* is smaller than the duration of the impulse response h (see Figure 3).

Next, we consider a Wilson basis of dimension 496. We choose

$$g_0(t) = \gamma_0(t) = \frac{1}{\sqrt{250}}\,\chi_{[0,250)}(t\,[\mu\text{s}])$$

with $M = 124$. The other parameters are chosen as in the Weyl–Heisenberg example. The channel matrix is shown in Fig. 9 and Fig. 10.

To obtain an exemplary wavelet system we shall use the orthogonal Daubechies wavelet with 4 vanishing moments, i.e., $g_0 =$ db4, scaled to support $[0, 1791]\mu s$ and normalized in the $L^2(\mathbb{R})$ sense. Furthermore, we set $T = 2^8 = 256\mu$s and $M = 8$ and obtain the transmission family

$$\{g_{k,m}^{(n)}(t)\}_{m=0,1,2,3,\ldots.8,\ n=0,1,\ldots.2^m-1,\ k\in\mathbb{Z}}.$$

The prototype function $g_0(t)$ is displayed in Figure 11. We reorder the orthonormal wavelet family according to

$$g_{511k+2^m-1+n}(t) = g_{k,m}^{(n)}(t).$$

A segment of the resulting effective channel matrix is displayed in Figure 12. The wavelet basis elements on the finest scale suffer the strongest orthogonal perturbation, reflecting their poor frequency localization.

Finally we consider a DS spread spectrum system based on a Walsh-Hadamard code. This modulation scheme is used in the North American cellular wireless system [14, p.849]. The transmission signal is given by

$$x(t) = \sum_k \sum_l c_{k,l} g^{(l)}(t - kT)$$

where $g^{(l)}(t)$ is the convolution of the binary-valued code sequence with index l and some bandlimited pulse-shaping signal. We consider this modulation scheme in a single-user setup, i.e., all of the $c_{k,l}$ contain information bits of the same user. (In the CDMA-type application of DS spread-spectrum l is the user index.) By

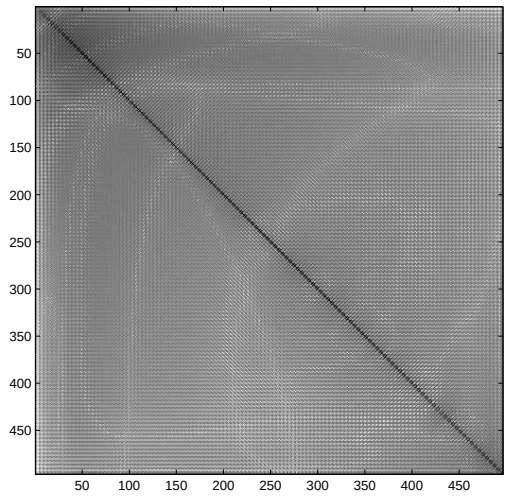

Fig. 9. Channel matrix of a OFDM/OQAM (Wilson-type family).

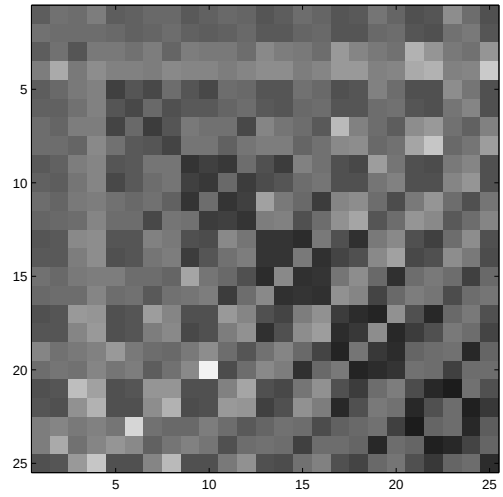

Fig. 10. Details of Figure 9.

the principle of spread-spectrum communication, the transmission components $g^{(l)}(t)$ deliberately have bad frequency-localization. Hence one must expect poor off–diagonal decay. Observe, however, that the robustness advantage of CDMA systems leads to a reduced variance of the diagonal elements (compared to OFDM where the diagonal elements correspond essentially to samples of $H(f)$).

Acknowledgements

Sponsoring by the German Ministry of Education and Science (BMBF) within the KOMNET program under grant 01 BP 902 is gratefully acknowledged.

6. REFERENCES

[1] J. A. C. BINGHAM, Multicarrier modulation for data transmission: an idea whose time has come. *IEEE Communications Magazine*, (1990), pp. 5-14.

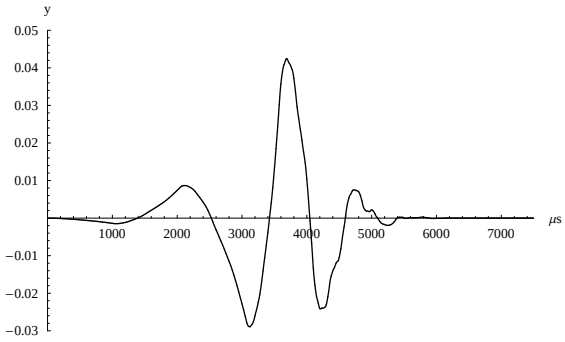

Fig. 11. g_0 in the wavelet basis.

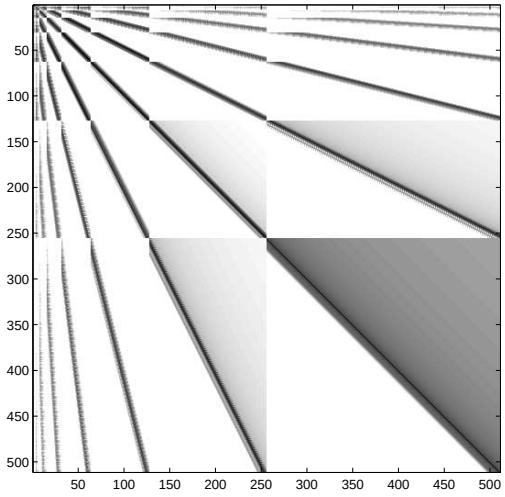

Fig. 12. Channel matrix of a wavelet family.

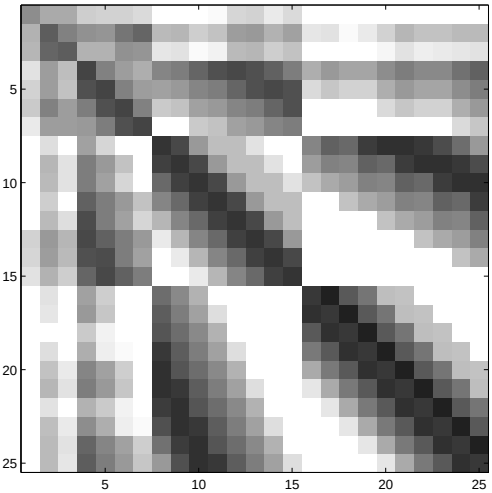

Fig. 13. Details of Figure 12

[2] H. BÖLCSKEI, P. DUHAMEL and R. HLEISS, Design of pulse shaping OFDM/OQAM systems for high data-rate transmission over wireless channels. In: *Proc. of IEEE Int. Conf. on Communications (ICC)*, Vancouver 1999, pp. 559–564.

[3] G. CHERUBINI, E. ELEFTHERIOU, S. OELCER, and J. M. CIOFFI, Filter bank modulation techniques for very high speed digital subscriber lines.

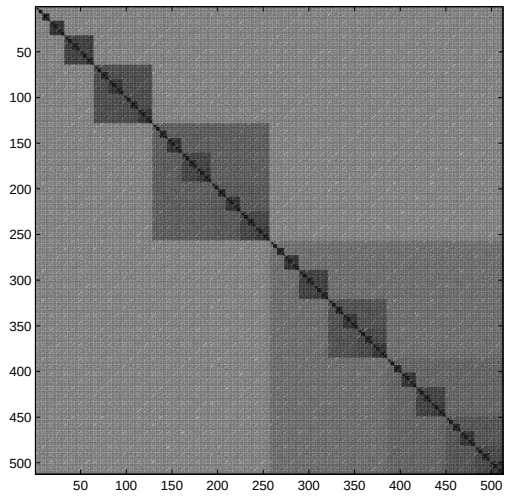

Fig. 14. Channel matrix for the Walsh-Hadamard system with N=512.

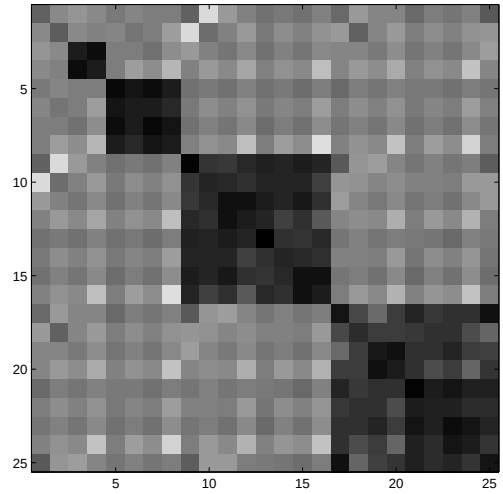

Fig. 15. Details of Figure 14.

IEEE Communications Magazine (2000), pp. 98–104.

[4] P. W. CHIN, Wavelet modulation for broadband networking connectivity: a business overview. *Rainmaker Technologies*, http://www.rainmakertechnologies.com/ tech_ white1.html, (2001).

[5] I. DAUBECHIES, *Ten Lectures on Wavelets* CBMS-NSF Lecture Notes Nr. **61**, SIAM, Philadelphia, 1992.

[6] EUROPEAN TELECOMMUNICATIONS STANDARDS INSTITUTE, Transmission and Multiplexing (TM); Asymmetric Digital Subscriber Line (ADSL); Requirements and performance, ETSI ETR **328** ed.1 (1996).

[7] W. KOZEK and A.F. MOLISCH, Nonorthogonal pulseshapes for multicarrier communications in doubly dispersive channels. *IEEE J. Selected Areas in Communications* **16** (1998), pp. 1579–1589.

[8] W. KOZEK, G. PFANDER, and G. ZIMMERMANN, Perturbation stability of coherent Riesz systems under convolution operators. *To appear in Applied and Computational Harmonic Analysis* (2002).

[9] A.R.. LINDSEY, Wavelet packet modulation for orthogonally multiplexed communication. *IEEE Trans. Sig. Proc* **45** (1997), pp. 1336–1339.

[10] A. RON, and Z. SHEN, Frames and stable bases for shift–invariant subspaces of $L_2(R^d)$, *Canadian Journal of Mathematics*, **47**, no.5, (1995), pp. 1051–1094.

[11] D. SLEPIAN and H.O. POLLAK, Prolate spheroidal wave functions, Fourier analysis and uncertainty — I. *Bell Syst. Tech. J.* **40** (1961), pp. 43–63.

[12] H.J. LANDAU and H.O. POLLAK, Prolate spheroidal wave functions, Fourier analysis and uncertainty — II. *Bell Syst. Tech. J.* **40** (1961), pp. 65–84.

[13] H.J. LANDAU and H.O. POLLAK, Prolate spheroidal wave functions, Fourier analysis and uncertainty — III: the dimension of the space of essentially time- and band-limited signals. *Bell Syst. Tech. J.* **41** (1962), pp. 1295–1336.

[14] J.G. PROAKIS *Digital Communications.* McGraw-Hill, New York, 1995.

[15] Y. MEYER, *Wavelets: Algorithms and Applications.* SIAM, Philadelphia, 1993.

[16] G. WORNELL, Emerging applications of multirate signal processing and wavelets in digital communications. *IEEE Proc.* **84** (1996), pp. 586–603.